Velocity of domain-wall motion during polarization reversal in ferroelectric thin films: Beyond Merz's Law

Qingping Meng, Myung-Geun Han, Jing Tao, Guangyong Xu, David O. Welch, and Yimei Zhu

Phys. Rev. B **91**, 054104 — Published 9 February 2015

DOI: 10.1103/PhysRevB.91.054104

The Velocity of Domain-Wall Motion during Polarization Reversal in Ferroelectric Thin-Films: Beyond Merz's Law

Qingping Meng[1, 2 *], Myung-Geun Han[1], Jing Tao[1], Guangyong Xu[1], David O. Welch[1], and Yimei Zhu[1 *]

[1]Department of Condensed Matter Physics and Materials Science, Brookhaven National Laboratory, Upton, New York 11973, USA

[2]School of Materials Science and Engineering, Shanghai Jiao Tong University, Shanghai 200030, China

The motion of domain walls (DWs) is critical to switching kinetics in ferroelectric (FE) materials. Merz's law, dependent only on the applied electric field, cannot explain recent experimental observations in FE thin films because these experiments showed that the DW velocity depend on not only the strength of applied electric field, but also size of reversal domain. In this paper, we derive a model to understand the dominant factors controlling the velocity of FE DWs. Our calculation reveals that the DW velocities are not only a function of the strength of the electric field, but also decay exponentially with increasing the characteristic time of the measurement, or the size of the growing domain. Our observations can naturally explain the gigantic variation reported in the literature, over 15 orders-of-magnitude, in the experimentally measured DW velocities, and the formation of the stripe shape of FE domains.

PACS numbers: 77.80.Fm, 68.35.Fx, 77.22.Ej

I. Introduction

Understanding how the motion of domain walls (DW) is driven by an applied electric field is the key to many applications involving ferroelectric (FE) materials, such as the incorporation of ferroelectric thin-film memories into standard silicon integrated circuits and high-density arrays of capacitors based on thin ferroelectric films [1, 2]. An electric field applied to a 180° DW will break the degeneracy of the ferroelectric double-well potential and lead to the motion of DWs during the reversal of polarization. Specifically, experimentally measured DW velocities have wide discrepancies, of up to 15 orders-of-magnitude ranging from 10^{-12} to 10^{3} m/s [3], for different measurement techniques. A summary of measured DW velocities in $Pb(Zr,Ti)O_3$ (PZT) thin film is listed in Table 1 [4-10]. Those DW velocities (the first column in Table 1) differ drastically even for the same materials (PZT) between different research groups.

A well-known empirical law, called Merz's law, has been widely employed to demonstrate the relationship between the DW velocity and the applied electric field: $v \propto \exp\left(-\frac{E_a}{E}\right)$, where E_a is the 'activation field' and E is the applied electric field [11]. For decades, Merz's law has been used and can correctly describe the trend of DW motion in bulk FE materials provided that the activation field is chosen properly [9, 12, 13]. In order to reveal the underlying physics of Merz's law, Miller and Weinreich [14] first developed a model for the DW velocity based on classical nucleation theory although experimental observations and theoretical calculations show that Miller and Weinreich's explanation overestimates the activation field by an order of magnitude [9, 12-13]. Miller and Weinreich suggested that the DW's motion in the presence of an applied electric field results from the repeated nucleation of steps along existing parent 180° DWs, and that their velocity is controlled by the nucleation rate [15]. This implies that the expansion of reversed domains is a process in which new reversed-domain nuclei continuously merge into a growth domain. The process described by Miller and Weinreich's model requires that there are sufficient nucleation centers in the sample. However, the existence of only limited

numbers of nucleation centers in FE thin films [16] leads to failure of this assumption of Miller and Weinreich's model. Therefore, Miller and Weinreich's explanation of Merz's law cannot adequately describe the DW velocity in FE thin films. Furthermore, the DW velocities in PZT thin films, shown in Table 1, reveal that they are not monotonically dependent upon the strength of the applied electric field (see the first and second column in Table 1) as indicated by Merz's law. This implies that other factors besides applied electric field also affect the DW velocity. We, as well as Scott and his collaborators in their recent review article [3], do not believe that so large a discrepancy (see the first column in Table 1) among the results of different researchers arises from the variations of the sample quality and the measurement technique. In contrast, variations of the characteristic time in various experimental methods, i.e., the averaged time resolution of a particular technique (see the third column in Table 1 and more detailed definition in the Supplementary Information), reveal a readily apparent trend of a significant decrease in velocity with increase of the characteristic time. This means that the DW velocities depend not only on the strength of applied electric field, but also on the characteristic time of the measurement [6, 8, 9]. Obviously, Merz's law cannot explain the relationship between DW velocity and the characteristic time because the time dimension was not taken into account. More importantly, there has been significant interest in experimentally measuring DW velocity during polarization reversal, in particular using aberration-corrected electron microscopy [17]. The gigantic variation in measured DW velocities has generated ever increasing confusion in the field of ferroelectrics and multiferroics. These considerations motivated us to develop a new theory of DW motion to account for these experimental results.

II. Formalism

In FE materials, the equivalently stable polarization states split into metastable- and stable-states under an applied electric field; thereafter, the metastable states decay, and the stable states nucleate and grow into metastable regions. Metiu et al [18] showed that this process can be described by the time-dependent Ginzburg-Landau equation. In this paper, we use this equation to discuss the motion of a 180° ferroelectric DW in an applied electric field. The free-energy density can be expressed as

$$F\left(P_i, P_{i,j}, \varepsilon_{kl}\right) = F_P\left(P_i\right) + F_{el}\left(\varepsilon_{kl}\right) + F_c\left(P_i, \varepsilon_{kl}\right) + F_E\left(E, P_i\right) + F_G\left(P_{i,j}\right) \quad (1)$$

where F_P and F_{el} are, respectively, the Taylor series expansions in powers of the spontaneous polarization $\mathbf{P} = \left(P_1, P_2, P_3\right)$ and the elastic strain $\left\{\varepsilon_{kl}\right\}$ ($k,l = 1,2,3$); F_c is the coupling energy between $\mathbf{P}$ and $\left\{\varepsilon_{kl}\right\}$. F_E is the energy associated with the applied electric field, E, in the direction of polarization, written as $F_E = EP$. F_G is the gradient energy due to the spatial variation of P within the domain-wall layer, viz., $F_G = \frac{1}{2} g_3 P_{,3}^2 + \frac{1}{2} g_1 \left(P_{,1}^2 + P_{,2}^2\right)$, where g_1 and g_3 are material-dependent constants; and $P_{,i} = \frac{\partial P}{\partial x_i}$. The sum of the first three terms in Eq. (1) is the free energy density, U, in the homogeneous phase without an applied electric field. In the tetragonal perovskite phase, polarization adopts the form $\mathbf{P} = \left(0,0,P_3\right)$. For simplicity, we use P instead of P_3; then the sum of the first three terms is

$$U = \alpha_1 P^2 + \alpha_{11} P^4 + \frac{1}{2} c_{11}\left(\varepsilon_{11}^2 + \varepsilon_{22}^2 + \varepsilon_{33}^2\right) + c_{12}\left(\varepsilon_{11}\varepsilon_{22} + \varepsilon_{11}\varepsilon_{33} + \varepsilon_{22}\varepsilon_{33}\right) - \left[B_1\varepsilon_{33} + B_2\left(\varepsilon_{11} + \varepsilon_{22}\right)\right]P^2 \quad (2)$$

We consider two kinds of 180° DWs (Fig. 1): (1) Transverse (or sidewise) (Fig. 1(a)); and, (2) longitudinal (or head-to-head) (Fig. 1(b)). The red arrow in Fig. 1 shows the orientation of applied electric field that is perpendicular to surface of thin film. In the transverse, P depends only on x_1; in the longitudinal, P depends only on x_3. In this paper, we will only consider a stress-free system, i.e., a system that is not clamped by surrounding medium. In the absence of stress $\sigma_{ij} = \frac{\partial F}{\partial \varepsilon_{ij}} = 0$, where the σ_{ij} is the Cauchy stress components, and using the elastic compatibility condition, all of the spontaneous strain components can be replaced by polarization [19]. The total free energy density can be simplified as follows:

$$F_i = \frac{1}{2}K_i P^2 + \frac{1}{4}A_i P^4 + EP + \frac{1}{2}g_i\left(\frac{\partial P}{\partial x_i}\right)^2 \quad \text{for } i\text{=1, 3;} \tag{3}$$

The subscripts i=1 and 3 in Eq. (3) respectively represent the transverse- and longitudinal-DW; the coefficients K_i and A_i are obtained using the method shown in ref. 19 (their explicit representations are given in the Supplementary Information).

According to the theory of Metiu et al [18], the most probable path from the metastable to the stable state that satisfies the time-dependent Ginzburg-Landau equation is

$$\gamma\frac{\partial P}{\partial t} = -\frac{\delta F}{\delta P} \tag{4}$$

where γ is the Landau-Khalatnikov damping-coefficient [20]. $\frac{\delta F}{\delta P}$ is the variational derivative of F with respect to P. Combining Eqs. (4) and (3), we obtain the following:

$$-\gamma\frac{\partial P}{\partial t} = -g_i\frac{\partial^2 P}{\partial x_i^2} + K_i P + A_i P^3 + E \qquad \text{for } i\text{=1, 3} \tag{5}$$

Referring the variables in Eq. (5) to moving coordinates, $z = x - vt$, Eq. (5) can be written as

$$\gamma v\frac{\partial P}{\partial z} + g_i\frac{\partial^2 P}{\partial z^2} - A_i\left(P - P_i^{(1)}\right)\left(P - P_i^{(2)}\right)\left(P - P_i^{(2)}\right) = 0 \tag{6}$$

Here, v represents the DW velocity, and $P_i^{(1)}$, $P_i^{(2)}$, and $P_i^{(3)}$ are the solutions of $A_i P^3 + K_i P + E = 0$. If $E < \frac{2}{3^{\frac{3}{2}}}A_i^{-\frac{1}{2}}\left(-K_i\right)^{\frac{3}{2}}$, the three roots are real, and they correspond to the polarization of the stable-,

unstable-, and metastable-states. Assuming that $P_i^{(1)} < P_i^{(2)} < P_i^{(3)}$, Eq. (6) has a solitary wave solution [18, 21]: $P(z) = P_i^{(1)} + \dfrac{P_i^{(3)} - P_i^{(1)}}{1+\exp(bz)}$ with $b = \left(P_i^{(3)} - P_i^{(1)}\right)\left(\dfrac{A_i}{2g_i}\right)^{\frac{1}{2}}$, and the DW velocity

$$v_i = \frac{1}{\gamma_i}\left(\frac{g_i A_i}{2}\right)^{\frac{1}{2}}\left(P_i^{(1)} + P_i^{(3)} - 2P_i^{(2)}\right) \tag{7}$$

If $E \neq 0$, one of the domains with polarization $P_i^{(1)}$ and $P_i^{(3)}$ will become metastable, whilst the other will remain stable. A transition from the metastable- to the stable-state will initiate the DW motion.

Eq. (7) has been obtained by some researchers [18, 21]. However, to evaluate the real DW velocity from Eq. (7), we require a knowledge of the value of γ_i. According to Landau and Khalatnikov's theory [20], γ_i is expressed as $\gamma_i = -2\mathrm{K}_i\tau_i$. τ_i is a unit of time and represents the relaxation time of polarization reversal from the metastable- to the stable-state crossed at the unstable-point $P_i^{(2)}$. This theory has been discussed by other researchers [22~26], and an approximation, as follows, was given by Caroli et al [26]:

$$\tau_i^{-1} = \left(\omega_i^{(3)}\omega_i^{(2)}\right)^{\frac{1}{2}}\exp\left(-\frac{\Delta U_i^{3-2}N}{k_B T}\right) + \left(\omega_i^{(1)}\omega_i^{(2)}\right)^{\frac{1}{2}}\exp\left(-\frac{\Delta U_i^{1-2}N}{k_B T}\right) \tag{8}$$

where $\omega_i^{(j)} = \left(\dfrac{\left|d^2U \big/ d\left(x_i^{(j)}\right)^2\right|}{m}\right)^{\frac{1}{2}}$; $x_i^{(j)}$ is the atomic displacement when the polarization equals $P_i^{(j)}$ (superscript *j*=1, 2, 3; they corresponds to three polarization state, $P_i^{(1)}$, $P_i^{(2)}$ and $P_i^{(3)}$); m is the effective atomic mass of the clusters of atoms that cross the energy-barriers; and $\omega_i^{(j)}$ represents the effective frequency of atomic vibration [22], and its typical value is about 20THz.

$\Delta U_i^{3-2} = U\left(P_i^{(2)}\right) - U\left(P_i^{(3)}\right)$ and $\Delta U_i^{1-2} = U\left(P_i^{(2)}\right) - U\left(P_i^{(1)}\right)$, which depend on strength of applied electric field, are the energy-barriers of the unstable-point $P_i^{(2)}$. N is the number of atomic clusters or molecules that flip from the metastable state to the stable one on domain boundary. For perovskite FE oxides, the atomic cluster is taken to be ABO_3. To calculate $d^2U \Big/ d\left(x_i^{(j)}\right)^2$, we use a linearized approximation [27], $P = \frac{e}{\Omega} z x_i^{(j)}$, where e is the absolute value of the electron charge, Ω is the unit cell volume, and z is the Born effective charge.

From the Landau theory, we know that the effective frequency ($\omega_i^{(j)}$) and the energy-barriers (ΔU_i^{3-2} and ΔU_i^{1-2}) of the unstable-point $P_i^{(2)}$ will decrease when the temperature approaches the critical point of ferroelectric phase transitions. τ_i^{-1} will decrease along with $\omega_i^{(j)}$, but increase with the decrease of ΔU_i^{3-2} and ΔU_i^{1-2} based on Eq. (8). Obviously, the effective frequency and the energy-barriers are determined by the nature of material and applied electric field. In this paper, we will focus on the effect of another factor, the characteristic time of the measurement, which is related to N in Eq. (8) and is independent of the nature of material and applied electric field.

III. Analysis and calculations

Using Eqs. (7) and (8), theoretically, the DW velocity can be calculated numerically for a given applied electric-field. However, these equations do not give an explicit relationship between the velocity of the DW and the intensity of the applied electric field because ΔU_i^{3-2} and ΔU_i^{1-2} in τ cannot be expressed by an analytical function of the strength of the electric field. Recently, some empirical formulae were suggested for the DW velocity derived from experimental results [8, 9, 28]. To compare our theory with these empirical formulae, some approximations to our theory are required so that the DW velocity can become an explicit function of the intensity of the electric field.

In order to obtain an explicit expression of the velocity of DW for the intensity of the electric field, we assumed that the applied electric field is small compared to $\frac{U_0}{P_0}$ (where $U_0 = \left|\frac{K_i^2}{4\mathrm{A}_i}\right|$ is the energy barrier between two equivalent states with $E = 0$, $\frac{U_0}{P_0} \approx 2\times10^6$V/cm for PZT, and typical applied electric fields are about 10^5V/cm. Therefore, the assumption is reasonable.). Using Taylor expansion, only keeping terms to first order in E, and neglecting reversed atomic flips from stable- to unstable-states we obtain

$$\tau_i^{-1} = ez\left(-\frac{\sqrt{2}K_i}{m\Omega}\right)^{\frac{1}{2}}\left(1+\frac{3E}{8K_iP_0}\right)\exp\left(\frac{N\left(P_0E-U_0\right)}{k_BT}\right) \tag{9}$$

Eq. (9) is similar to the result obtained by Griffiths et al [23]. From Eq. (9), we find that the DW velocity is zero as long as $E < \frac{U_0}{P_0}$ at $T = 0$, whereas for $E > \frac{U_0}{P_0}$, the DW starts moving. The action of $\frac{U_0}{P_0}$ is similar to a threshold force for a pinning-depinning transition [29, 30]. For $E << \frac{U_0}{P_0}$ and $T \neq 0$, the DW velocity generated by an applied electric field can be written as:

$$v_i = 2^{-\frac{5}{4}}\left(-\frac{g_iA_i}{K_i^2m\Omega}\right)^{\frac{1}{2}}ezE\exp\left[-\frac{NU_0}{k_BT}\cdot\frac{\frac{U_0}{P_0}}{\frac{U_0}{P_0}+E}\right] \tag{10}$$

When we merge all constants together, Eq. (10) can be further simplified.

$$v_i = f_iE\exp\left[-\frac{L}{k_BT}\cdot\frac{f_0}{E_0+E}\right] \qquad (i = 1, \text{ or } 3) \tag{11}$$

where $f_0 = \frac{U_0^2}{aP_0}$, $E_0 = \frac{U_0}{P_0}$ and $f_i = 2^{-\frac{5}{4}}\left(-\frac{g_i A_i}{K_i^2 m\Omega}\right)^{\frac{1}{2}} ez$ are constants dependent on material; $L = Na$ (here a is lattice constant) represents the DW width. Obviously, the width of domain wall L is in directly proportional to the size of reversed domain. Eq. (11) is similar to Eq. (5) of Ref. 28, which was derived from experimental data, but a physical expression for the threshold electric field $E_0 = \frac{U_0}{P_0}$ was not given therein.

The DW velocity from Eq. (11) differs from the Merz's law [11, 14]. This is not surprising because our theoretical model envisions the DW motion as "jumps" of atomic clusters driven by applied electric-field while Merz's law was derived via a classical nucleation model. The jumping probability of atomic clusters strongly depends on the barrier's height. Its height for $E = 0$ is $U_0 = \left|\frac{K_i^2}{4\mathrm{A}_i}\right|$. Because $P_0 = \left(-\frac{K_1}{A_1}\right)^{\frac{1}{2}} = \left(-\frac{K_3}{A_3}\right)^{\frac{1}{2}}$ [19], the difference between K_1 and K_3 (see Supplementary Information) results in the different U_0 in $i = 1$ and 3 orientation, therefore, lead to the different velocities of the longitudinal- and transverse-DWs.

From Eq. (11), we note that the velocity of DW depends on the DW width, and thus it will be a function of the domain's size. This result was confirmed in experiments using atomic-force microscopy and piezo-response force microscopy [5, 6, 9, 31, 32] and atomistic simulations [33]. Experiments carried out by Tybell et al [9] and Dawber et al [32] indicated that the reversed domain size, r, increases logarithmically with increasing writing time, t, of the applied electric field, i.e., $r \propto \ln t$. Using this result, we easily obtain $v \propto \exp(-Cr)$, where C is a constant independent of t. If the applied electric field is fixed, Eq. (11) can be written as $v = v_{i0}\exp(-Cr)$, where v_{i0} and C are the constants related to the applied electric field and material. This result is consistent with experimental observations.

For illustrating our theory, we calculated the DW velocity in $Pb(Zr_{0.2}Ti_{0.8})O_3$ as an example, using the parameters [34] in our calculation taken from Refs [27, 35~36]. The coefficients of the gradient energy were determined by the thickness of DW, based on high-resolution transmission electron microscopic imaging [37].

Fig. 2 shows the calculated DW velocity versus nucleus size for various applied electric fields using Eqs. (7) and (8). The velocity of a longitudinal DW is much higher than that of a transverse DW under the same applied electric field. This finding means that the energy barrier of a longitudinal DW is smaller than that of a transverse DW. The curves in Fig. 2 are almost linear when the scale of velocity is logarithmic, implying that the velocity can be approximated as $v \propto \exp(-Cr)$, consistent with the experimental observations[31, 32]. The coefficient C depends on the strength of electric field for a specific material. The DW velocities in Fig. 2 have a very large range depending on the size of growing domains. As is also evident therein, the growth of the nucleus is extremely rapid (~ 10^3m/s) in its early stage, and then slows down exponentially as the domain size increases. Table 1 lists the DW velocity in PZT from experiments measured by various researchers; the data show clearly that velocity depends sensitively upon the characteristic time of the experimental measurements. Experimentally, typical measurements of the switching kinetics in FE thin film use voltage pulses to supply the applied electric field. The DW velocities are determined by $v = \Delta r / \Delta t$ (where Δr is an increment of domain size, and Δt is the width of voltage pulse, i.e., characteristic time of measurements). Our theory indicates that the DW velocity has generally instantaneous differential characteristics during the growth of reversed domain, even when the strength of applied electric field is fixed. Therefore, the above measured method gives only an average DW velocity. Because the instant velocity exponentially decreases with the increase of the growth of reversed domain, the average velocity rapidly drops with increasing global measurement time Δt. For that reason, the shorter is Δt, the larger is the averaged velocity will be

measured. A similar trend of the DW velocity is seen in Table 1 and Fig. 3, consistent with our theoretical prediction.

As mentioned above, Merz's law describes the DW velocity when it is controlled by the aggregation kinetics of nuclei of reversed domain. Unlike the Merz's law, the velocity described by this paper depends on not only applied electric field, but also the size of reversed domain. Based on our theory, the velocity will quickly become immeasurably small with increasing nucleus size. At that time, our mechanism accounting for the DW motion becomes inapplicable; instead, the nucleation mechanism for DW motion, namely, the Merz's law, will prevail. Thus, two mechanisms will control the domain switching kinetics. Which one is primarily responsible depends on the competition between nucleation rate and nucleus self-growth of reversed domains. Because of a significant number of nucleation rates in bulk FEs, these nuclei of reversed domain form and merge, and then lead to propagation of reversed domain. In this case, the DW velocity is expressed in terms of the nucleation rate [15], i.e., the velocity corresponds to the Merz's law. Conversely, for FE thin films, the nucleation sites of reversed domain are limited [16, 28]. In this case, the expansion of reversed domain only depends on the self-growth of these limited nuclei, and the DW velocity can be explained by our theory. Two experimental findings support this conclusion. 1) Based on nucleation-limited switching (NLS) model [16] in FE thin films, Jo et al [28] obtained an empirical formula for the DW velocity from their experimental results. Their empirical formula is similar to our Eq. (11). 2) Gruverman et al's experiment [6] demonstrated that the deceleration of propagation of the domain wall, with the switching behavior obeying the NLS model, depends logarithmically on their measurement time. This time-dependence corresponds naturally to our model which takes into account the effect of increasing nuclei sizes on the DW velocity.

During switching, a stripe shape of the reversed domains is often observed [11, 14, 38]. Miller and Weinerich [14], and Fatuzzo [38] using Merz's law only explained the transverse motion of DW, but not longitudinal motion. Here, we offer an explanation by the application of our theory. First, we use a two-dimensional triangular nucleus model [14, 15] to describe the shape of an initial nucleus of a reversed

domain. Fig. 2 shows $v \propto \exp(-Cr)$ is a very good approximation. Using the approximation, the velocities in x_1 (transverse) and x_3 (longitudinal) orientation are

$$\frac{dx_1}{dt} = 2v_{10}\exp(-C_1 x_3) \tag{12a}$$

$$\frac{dx_3}{dt} = v_{30}\exp(-C_3 x_1) \tag{12b}$$

where v_{10}, v_{30}, C_1 and C_3 are material constants which depend upon the intensity of the applied electric field and temperature and are obtained by means of the fitting of the curve in Fig. 2.

The basic characteristic of the solutions of Eq. (12) is that the expansion of one orientation will predominate, while that of another orientation will be restrained. Therefore, the reversed domain will grow as a narrow stripe. Numerical study shows that small changes of v_{10}, v_{30}, C_1, C_3, and of the initial condition will lead to a large change in the solution of Eq. (12). Usually, we have $C_3 < C_1$ and $v_{30} > v_{10}$ for a given electric field in PZT (for example, $C_1 \approx 1.5112$, $C_3 \approx 1.1476$, and $v_{10} \approx 2346.61$, $v_{30} \approx 7752.23$ when the applied electric field is 500KV/cm), so that longitudinal expansion will predominate in most cases, as has been observed in many FEs not only in the PZT [11, 15]. However, the inhomogeneous strain field and electric fields between the FE film and substrate can change v_{10}, v_{30}, C_1, C_3, and the shape of initial nuclei, which also can cause predominant expansion of reversed domain in the transverse direction, as recently was observed experimentally [39]. Fig. 3 shows a calculated example that the triangular nucleus develops into a stripe domain for an applied electric field of 500KV/cm. Fig. 4 shows the DW velocity of a triangular nucleus versus characteristic time of measurement. From Fig. 4, we see that the expansions of nuclei already have larger longitudinal velocity than transverse velocity at the beginning stage of growth, and the difference becomes more pronounced over time. Finally, the longitudinal velocity approaches a constant, and the velocity along the transverse direction will be close

to zero, and a stripe domain comes into being. After the formation of a stripe domain, the DW's sidewise velocity predicted by our theory is zero. It means that our theory will fail to predict the sidewise velocity at this time. Merz's law will replace our theory to describe the sidewise velocity [14, 38].

The experimental data in Table 1 are also shown in the Fig. 4. Comparison of our theory with the experimental results shows that our theory can give a good account of the variation of DW velocity with characteristic time of measurement. However, the experimental results appear 1 to 2 orders of magnitude larger than our calculation for short of values of characteristic time of measurement. Some important factors can lead to the discrepancy. First, the nuclei of reversed domains form preferentially in defect areas where the reversed domains are energetically favorable, and the original domains stay in the higher energy state during the reversal of polarization. These effects of nucleation in defect areas are equivalent to decreasing the energy barrier and increasing the applied electric field. Undoubtedly, they will exponentially enhance the DW velocity in the nucleation stage. Second, many experiments show (see Supplementary Information) that the nuclei of reversed domain in thin ferroelectric film are much to form at the interface of ferroelectric and substrate. One reason is that the interface is a natural defect; another important reason is a depolarizing field effect due to the interface. According to Kretschmer and Binder's calculation [40], an important contribution of the depolarizing field effect is to decrease the absolute value of the coefficient K_i of Landau polynomial. The decrease of the absolute value of K_i will quadratically decrease the energy barrier $U_0 = \left| \frac{K_i^2}{4\mathrm{A}_i} \right|$. It means that the DW velocity of the nuclei formed on the interface will be much larger than our prediction. Third, ferroelectric-electrode coupling may lead to the existence of favorable conditions for reverse domain nucleation and significantly decrease the coercive field [41]. All of these imply that the DW velocity from our calculation in nucleation stage was possibly underestimated. Some factors also decrease the DW velocity. For example, the depolarizing energy due to the divergence of polarization at the domain boundary will increase the nucleation barrier [14, 41]; defects can block DW motion; and the free charge compensation of the bound polarization charge can

cause a substantial reduction of the domain wall mobility [42]. All in all then, many factors will affect the DW velocity so that the calculation of the velocity becomes too complex to estimate an accurate value. Only an intrinsic velocity with a correct trend was given in this paper.

IV. Conclusions

In summary, we have developed a theoretical model that predicts the longitudinal- and transverse-DW velocities in ferroelectrics under an applied electric field. We found a dominance of the size effect, or the characteristic time effect, over the effects of the applied electric field on the velocities of DWs. Our theoretical analyses address the large variation in experimental data, which can now be attributed to the dependence of DW velocity on growing domain size. The anisotropy of DW velocities found in our model also explains the formation of FE stripe domains. When the switching kinetics in FE thin film obeys the NLS model, the DW's velocity can be described by our theory.

Acknowledgments

The work was supported by U. S. Department of Energy, Office of Basic Energy Science, under Contract No. DE-AC02-98CH10886. Q. M. acknowledges Chinese NNSF (No. 50471014) for partial support.

* Author to whom correspondence should be addressed. Email: qmeng@bnl.gov, and zhu@bnl.gov.

References:

1. J. F. Scott, and C. A. Paz de Araujo, Science 246, 1400(1989).
2. M. Dawber, K. M. Rabe, J. F. Scott, Rev. Mod. Phys. 77, 1083(2005).
3. G. Catalan, J. Seidel, R. Ramesh, J. F. Scott, Rev. Mod. Phys. 84, 119 (2012).
4. J. Li, B. Nagaraj, H. Liang, W. Cao, Chi. H. Lee, and R. Ramesh, Appl. Phys. Lett. 84, 1174(2004).
5. A. Grigoriev, D. -H. Do, D. M. Kim, Ch.-B. Eom, B. Adams, E. M. Dufresne, and P. G. Evans, Phys. Rev. Lett. 96, 187601(2006).
6. A. Gruverman, D. Wu, and J. F. Scott, Phys. Rev. Lett. 100, 097601(2008).

7. A. Gruverman, B. J. Rodriguez, C. Dehoff, J. D. Waldrep, A. I. Kingon, and R. J. Nemanich, J. S. Cross, Appl. Phys. Lett. 87, 082902(2005).

8. J. Y. Jo, S. M. Yang, T. H. Kim, H. N. Lee, J.-G. Yoon, S. Park, Y. Jo, M. H. Jung, and T. W. Noh, Phys. Rev. Lett. 102, 045701(2009); S. M. Yang, J. Y. Jo, D. J. Kim, H. Hung, T. W. Noh, H. N. Lee, J. -G. Yoon, and T. K. Song, Appl. Phys. Lett. 92, 252901(2008); D. J. Kim, J. Y. Jo, Y. S. Kim, and T. K. Song, J. Phys. D 43, 395403(2010).

9. T. Tybell, P. Paruch, T. Giamarchi, and J. -M. Triscone, Phys. Rev. Lett. 89, 097601(2002).

10. Myung-Geun Han: TEM measurement at Brookhaven National Laboratory was located in Supplementary Information.

11. W. J. Merz, Phys. Rev. 95, 690(1954).

12. J. Padilla, W. Zhong, and D. Vanderbilt, Phys. Rev. B53, R5969(1996).

13. Y.-H. Shin, I. Grinberg, I.-W, Chen, and A. M. Rappe, Nature, 449, 881(2007).

14. R. C. Miller and G. Weinreich, Phys. Rev. 117, 1460(1960).

15. M. Hayashi, J. Phys. Soc. Japan 33, 616(1972).

16. A. K. Tagantsev, I. Stolichnov, N. Setter, J. S. Cross, and M. Tsukada, Phys. Rev. B 66, 214109(2002).

17. P. Gao, C. T. Nelson, J. R. Jokisaari, S.-H. Baek, C. W. Bark, Y. Zhang, E. Wang, D. G. Schlom, C.-B. Eorm, and X. Pan, Nat. Commun. 2, 591(2011).

18. H. Metiu, K. Kitahara, and J. Ross, J. Chem. Phys. 64, 292-299(1976).

19. W. Cao and J. E. Cross, Phys. Rev. B44, 5(1991); W. Cao and G. R. Barsch, Phys. Rev. B41, 4334(1990).

20. L. D. Landau and I. M. Khalatnikov, Collected papers of L. D. Landau, ed. D. ter Haar, New York, Gordon and Breach, 1965, p. 626.

21. M. A. Collins, A. Blumen, J. F. Currie, and J. Ross, Phys. Rev. B19, 3630(1979).

22. R. Landauer and J. A. Swanson, Phys. Rev. 121, 1668(1961).

23. R. B. Griffiths, G. Y. Weng, and J. S. Langer, Phys. Rev. 149, 301(1966).

24. K. Kitahara, H. Metiu, and J. Ross, J. Chem. Phys. 63, 3156(1975).

25. Y. Saito, J. Phys. Soc. Jpn. 41, 388(1976).

26. B. Caroli, C. Caroli, and B. Roulet, J. Stat. Phys. 21, 415(1979).

27. O. Diéguez, K. M. Rabe, and D. Vanderbilt, Phys. Rev. B, 144101(2005).

28. J. Y. Jo, H. S. Han, J.-G. Yoon, T. K. Song, S.-H. Kim, and T. W. Noh, Phys. Rev. Lett. 99, 267602(2007).

29. P. Chauve, T. Giamarchi, and P. Le Doussal, Phys. Rev. B 62, 6241(2000).

30. M. Müller, D. A. Gorokhov, and G. Blatter, Phys. Rev. B 63, 184305(2001).

31. P. Paruch, T. Tybell, and J. -M. Triscone, Appl. Phys. Lett. 79, 530(2001).

32. M. Dawber, D. J. Jung, J. F. Scott, Appl. Phys. Lett. 82, 436(2003).

33. Q. Zhang, R. Herchig, and I. Ponomareva, Phys. Rev. Lett. 107, 177601(2011).

34. The list of the parameters of free energy used in the calculations for PZT (in SI unit, the temperature T in K): $\alpha_1 = 4.74(T - 567.4)\times 10^5$, $\alpha_{11} = 44.99\times 10^7$ (α_1 , and α_{11} were recalculated based on the data of ref. 34. Because we use four-power polynomial, six-power polynomial was used in ref. 28), $B_1 = 7.151\times 10^9$, $B_2 = -3.296\times 10^9$, $c_{11} = 2.585\times 10^{11}$, $c_{12} = 1.508\times 10^{11}$. Lattice constant: a =0.3953nm, c =0.4148nm, the Born effective charge $z = 8.78$.

35. A. Amin, R. E. Newnham, and L. E. Cross, Phys. Rev. B 34, 1595(1986).

36. J. Frantti, J. Lappalainen, D. Eriksson, V. Lantto, S. Nishio, M. Kakihana, S. Ivanov, and H. Rundlöf, Jpn. J. Appl. Phys. 39, 5697(2000).

37. Myung-Geun Han (unpublished): HRTEM measurement at Brookhaven National Laboratory revealed that the thicknesses of a DW were, respectively, 7- and 25-lattice constants in the x_1 direction, and the x_3 direction. Some others also gave their measured results, such as C. Jia, S. Mi, K. Urban, I. Vrejoiu, M. Alexe, and D. Hesse, Nature Materials, 7, 57(2008) and theoretical calculation, B. Meyer and D. Vanderbilt, Phys. Rev. B 65, 104111(2002). They have somewhat different results, but these differences do not change our calculated results significantly.

38. E. Fatuzzo, Phys. Rev. 127, 1999(1962).

39. C. T. Nelson, P. Gao, J. R. Jokisaari, C. Heikes, C. Adamo, A. Melville, S. Baek, C. M. Folkman, B. Winchester, Y. Gu, Y. Liu, K. Zhang, E. Wang, J. Li, L. Chen, C. Eom, D. G. Schlom, X. Pan, Science, 334, 968(2011).

40. R. Kretschmer, and K. Binder, Phys. Rev. B 20, 1065(1979).

41. G. Gerra, A. K. Tagantsev, and N. Setter, Phys. Rev. Lett., 94, 107602(2005).

42. P. Mokrý, A. K. Tagantsev, and J. Fousek, Phys. Rev. B 75, 094110(2007).

Table 1 The experimentally measured velocities of DW motion in PZT

Velocity (m/s)	Electric field kV/cm	The characteristic time of the measurement Δt	References
2000~3000	250	~80ps	4
40	450	620ps	5
10~100	100	100ns	6
0.3~0.4	78	220ns	7
0.02~0.04	600	1 μs	8
10^{-8}~10^{-2}	700~5000	50μs; 1ms; 100ms	9
~10^{-6}	260~1000	100ms	10

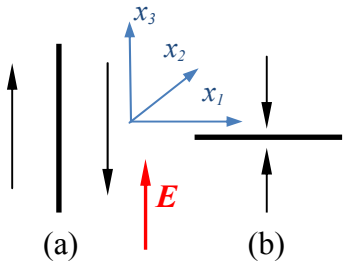

FIG. 1. Two kind of 180 domain wall: (a) transverse domain wall and (b) longitudinal or head-to head domain wall. Orientation of spontaneous polarization with respect to the wall and that of applied electric field is shown with black and red arrows.

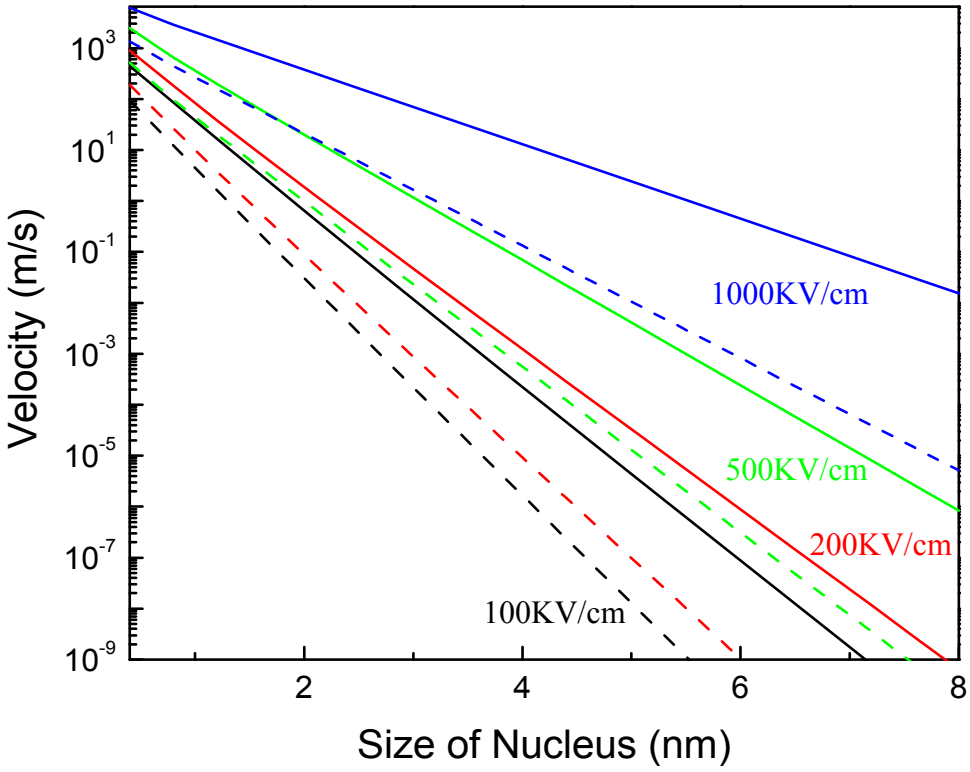

FIG. 2 The calculated velocity of DW motion versus size of nucleus for various values of applied electric field E=100 (black line), 200 (red line), 500 (green line) and 1000KV/cm (blue line). Solid lines are longitudinal velocity, and dashed lines are transverse velocity.

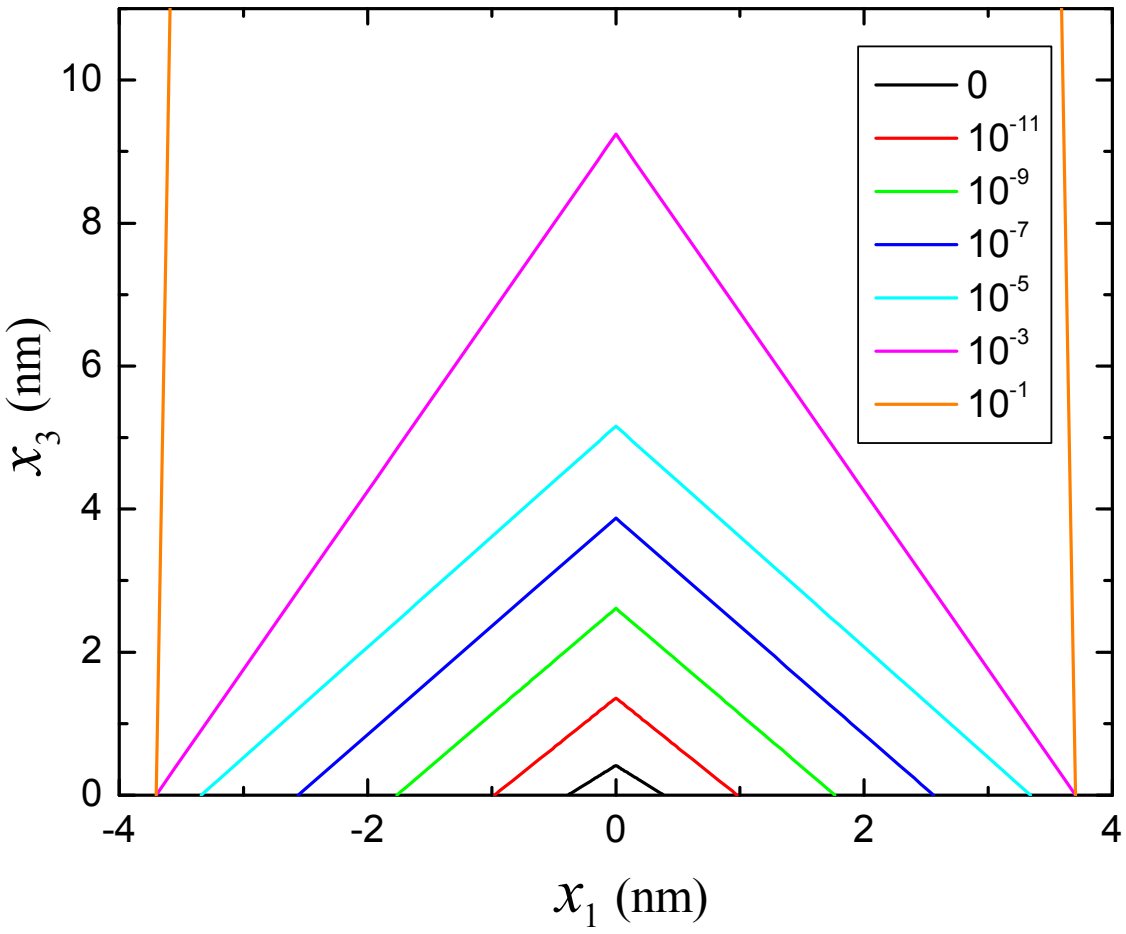

FIG. 3 (color online). (a) The evolution of a triangular nucleus in an applied electric field 500KV/cm. The base and attitude of the initial triangular nucleus are respectively about 2 and 1 lattice cells.

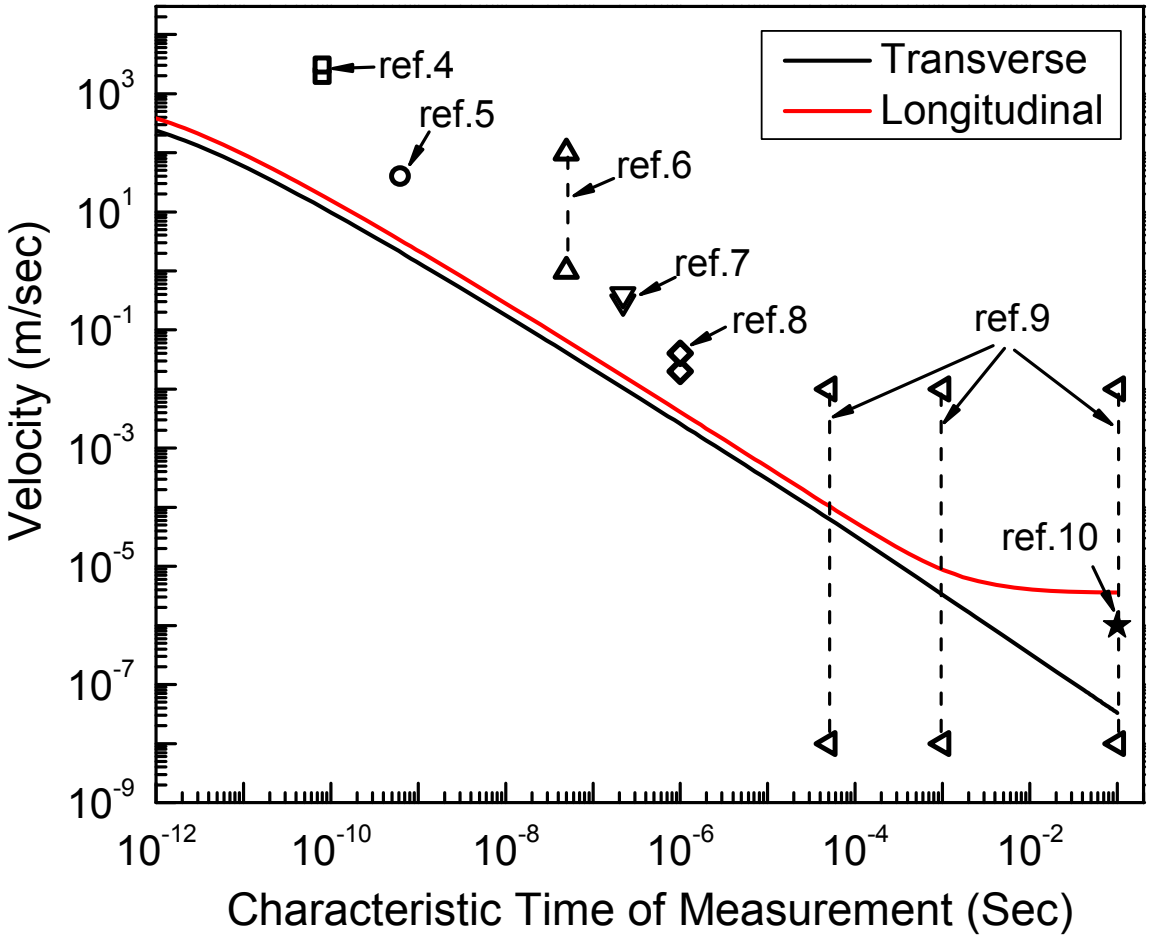

FIG. 4 (color online). The calculated DW velocity versus characteristic time of the measurement based on our new theoretical model. For comparison, experimental measurements listed in Table 1 from several literatures are also included with different symbols. The three data sets from ref.5 with the upper and lower values represent the range of the measured DW velocities due to the variation in the samples, the strength of applied electric fields and the characteristic time of the measurement.